

# Metal Object Localisation and Discrimination by Extended Symmetry and Phase Features

Hartmut EIGENBROD, Fraunhofer IPA, Stuttgart, Germany

**Abstract.** Handheld metal detectors are one of the most common devices used for clearing landmines in the context of humanitarian demining. However, their capability to discriminate between different objects is limited, leading to a high false alarm rate. In this work, data sets from spatially referenced measurements with an induction detector are evaluated. First, regions of interest are identified by a new method that considers signal symmetry in combination with classical threshold based methods. Second, a new approach of applying phase plots to discriminate buried objects is presented that applies to multi-frequency continuous wave metal detectors. Multidimensional phase observables are constructed that allow successful subsequent classification. The capability of the new methods is demonstrated using data sets from numerical simulations as well as from different test lanes. The achieved improvements in the field of object discrimination are presented.

## 1 Introduction

As a legacy of armed conflicts land mines endanger the population in many countries. The rapid and complete removal of the about 100 million buried land mines world-wide is a large technical challenge. At present, the most frequently used device for humanitarian demining is the metal detector [1]. The prevalence of this type of device has several reasons: Metal detectors are sensible for very small metal pieces, well suited for rough areas, easy to use and cheap. However, metal detectors can not distinguish between dangerous mines and unoffending objects that pervasively exist in the ground. As a result, metal detectors exhibit a high false alarm rate.

Deminers in the field estimate that for each true landmine alarm there are about 400 false alarms from harmless objects. As every indicated object has to be excavated by the deminer, the high false alarm rate slows down the demining process significantly. In addition, too many false alarms may lead to an inattentive behaviour in the mine field. Therefore, one main objective in metal detector research in the context of humanitarian demining is to reduce the high false alarm rate. When this objective is addressed by signal analysis methods the idea is to extract additional information from raw data and to subsequently classify unknown objects in the two categories “object is possibly a mine” and “object is definitely not a mine”.

One promising approach is to expand the data basis and to use spatially referenced data sets. This considers the fact that adjacent measurement values are highly correlated when a detector is moved over an object. In practice, there are different techniques available for a simultaneous measurement of the position: The metal detector could be mounted on a x-y-scanner that is moved over an area on a regular pattern. This method for example is used on different test lanes imitating a mine field [2, 3]. In another approach, handheld metal detectors are enhanced by a position measuring device, like a camera-based system detecting reference points [4] or calculating correlations [5].

A metal detector enhanced with a position sensor provides an increased amount of raw data. To extract the relevant information, new signal analysis algorithms are necessary. First, the signals have to be scanned for buried metallic objects to obtain regions that are then evaluated in more detail. Currently, this task is done manually by the deminer in the field. The metal detectors in use measure induction voltages and alert the deminer when the value is over a certain threshold. The deminer then estimates the exact position of the mine by a so called “pin-pointing” procedure [1]: The detector is swept on different pathways over the mine monitoring the acoustic alarm. As a result, the estimated closest position to the mine is marked.

Secondly, instead of excavating objects in question the signals in the vicinity of that object are evaluated. The objective is to find features that allow for object discrimination or at least a distinction in the two categories “object is possibly a mine” and “object is definitely not a mine”. One approach is based on the evaluation of the complex responses of continuous wave (CW) metal detectors [6, 7]. In that context, especially phase values have shown their capability for object discrimination as shown by Bruschini et al. [7]. Here, based on the results of a computer simulation, the in-phase and quadrature signal components for different frequencies are combined to multidimensional phase values.

In this paper, new algorithms for automated pin-pointing and for object discrimination are presented. The pin-pointing algorithm evaluates symmetry features in spatially resolved data sets, in combination with the classical threshold based approach. The object discrimination is based on characteristic 2d phase values that are calculated for unknown pin-pointed objects.

## 2 Automated Pin-Pointing

When a metal detector is combined with a position measuring device, the resulting enhanced metal detector provides 2d data sets representing the trajectory. An obvious additional feature in these data sets is the symmetry around objects in question. In Fig. 1, a simulated 2d data set for a measurement with a receiving coil in double-D configuration is shown (details of the simulation are given in chapter 2.2). The signal that is measured around the object is anti-symmetric regarding a  $180^\circ$  rotation around the centre of the object. This kind of symmetry holds for all spherical objects and it is a good approximation for other small objects. Similar symmetries exist for detectors with elliptic coils as well.

### 2.1 Description of the algorithm

The new algorithm for automated pin-pointing extends the classical threshold based approach by evaluating the symmetry in the data sets. The combination of these two criteria improves the ability to detect metal objects as will be shown in this chapter.

An algorithm for detecting symmetry in the context of humanitarian demining has to possess the following two properties: First, it has to detect the symmetry independently from the contrast in order to cope with different depths. As the signal strength drops with the 6<sup>th</sup> power of the objects depth due to the Maxwell Equations, differences in signal strength between shallow and deep objects easily reach magnitudes of  $10^3$  or higher. Secondly, the algorithm has to point the centre of the object as close as possible. Thereby, the algorithm provides a reliable reference point for subsequent feature extractions.

The new algorithm for detecting symmetry is based on metal detector data sets on a regular 2d grid. It works with data sets from CW metal detectors as well as with datasets from pulse induction detectors when in the later case the time response at one position is condensed to a single value. Often, this is accomplished by integrated the time response in a window of interest. In the following, the algorithm is described for signals that are

recorded with a metal detector having a double-D receiving coil. The results, however, could easily be transferred to other designs. The algorithm is as follows:

$$\text{symm}(S) = \text{onepass}(\text{grad}_x(\log(\text{onepass}(S)))) \quad (1)$$

$$\text{with } \text{onepass}_{i,j}(S) = \sum_{\substack{k \in \{-n, -n+1, \dots, n\} \\ l \in \{1, 2, \dots, n\}}} (S_{i+k, j+l} + S_{i-k, j-l} - 2S_{i,j})^2 \quad (2)$$

The recorded data set is stored in a 2d array with entries labelled  $S_{i,j}$ . The parameter  $n$  denotes the window size for the symmetry operation. For optimal results, this parameter has to be chosen subject to the coil size. The gradient is taken perpendicular to the symmetry axis of the receiving coil, as shown in Fig. 1. Spatially smoothing of the data set typically enhances the result on noisy data sets. Therefore, a mean filter or a 2d Butterworth low-pass filter is usually applied in advance. Moreover, the results could be improved by prior applying methods for soil compensations, e.g. different methods for multivariate data sets.

## 2.2 Results for simulated 2d data sets

The new algorithm is first evaluated using data sets from numerical simulations. In this way, the capability of the algorithm is shown independently from disturbing effects, like e.g. variations in the soil composition. The simulations are performed by a computer program of the University of Köln [8] that is based on a dipole approximation for small metallic spheres. The configuration for the simulation consists of two steel spheres with diameter 10 mm. They are located in the x-y-plane at the positions (30 cm, 30 cm) and (90 cm, 30 cm), lying 5 cm resp. 10 cm below the detector. The excitation frequency is 2.400 Hz. The induction values are computed for a regular grid with a mesh size of 2 mm and scaled by a uniform factor. The data sets from the simulation are shown in Fig. 1.

At first, two standard symmetry algorithms from the field of image processing are applied to the simulated data sets. In both cases, the simulated data sets are converted to fulfil the symmetry assumptions of the algorithms (rotational symmetry, established by integration in the data sets along the x-axis). Moreover, the values are linearly transformed to the interval [0:255] as the image processing algorithms are typically optimized for this range.

The algorithm of Reisfeld et al. [9] localizes the object with high contrast, but fails in detecting the low contrast object on the right (Fig. 2). Even when methods for contrast enhancement are applied, like log-scale transformations of the data set, this shortcoming is still existent. On the other hand, the localisation of the shallow object works in principle although it is not perfect. The algorithm of Kovési [10] detects objects with different contrasts as can be seen in Fig. 3. However, the localisation resp. pin-pointing for symmetric objects is not satisfying: There is no sharp peak that marks the centre of the objects. Due to the described restrictions, both algorithms are unsuitable for automated pin-pointing of metallic objects.

The result of the automated pin-pointing algorithm, equation (1), is shown in Fig. 4. The two metal spheres are well localised by two dark spots, i.e. the spots have the correct x-y-positions and their boundaries are sharp. The influence of the contrast on the spot intensity and geometry is very small. These good results could be ascribed to the construction of the algorithm: The tight localisation is due to the twofold application of the symmetry operation in equation (2). The independence of the contrast is due to the intermediate operation  $\text{grad}(\log)$ .

The improvement of the new pin-pointing algorithm based on symmetry is obvious. In addition, further precision could be achieved by applying centre-of-mass algorithms for

sub-pixeling the x-y-position. By another extension, the additional spot with lower intensity exactly in the middle between the two dominating spots could be eliminated.

Fig. 1: Simulated measurement data for a CW metal detector with a receiving coil in double-D geometry. The scene contains two steel spheres at depth 5 cm (left) and 10 cm (right). The values shown are the induction voltages.

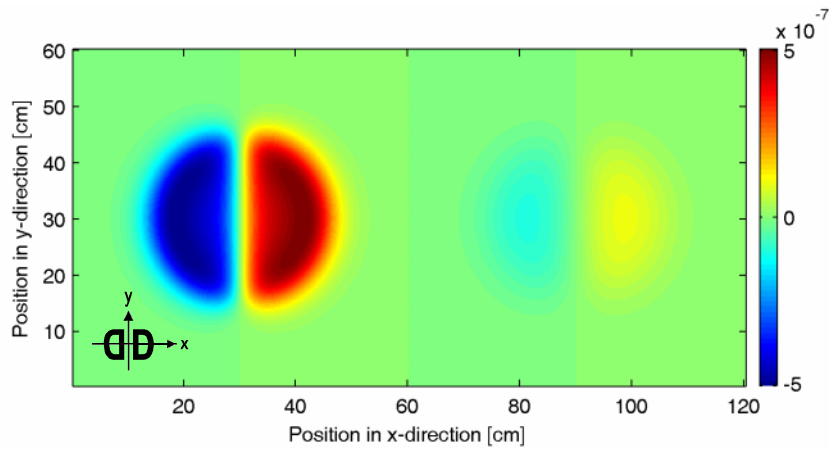


Fig. 2: Results of the symmetry operator  $S_1(p,1)$  from Reisfeld et al. Only the left object with high contrast is found.

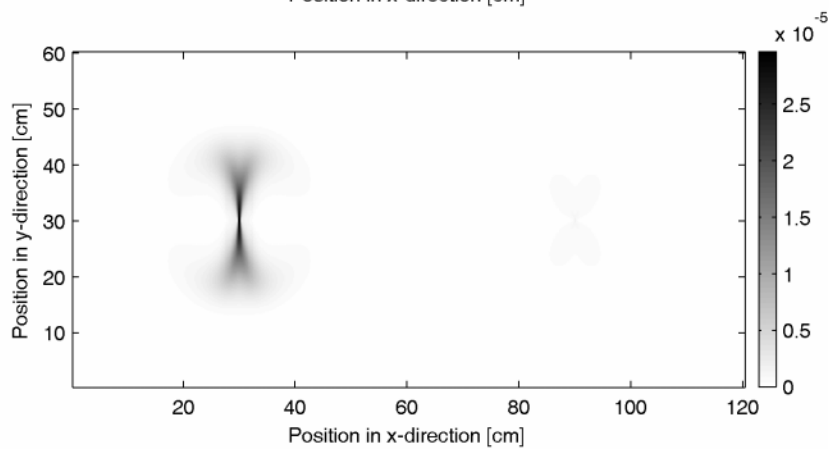


Fig. 3: Results of the symmetry operator from Kovesi. Both objects are found. However, the indications of the object centres are blurred.

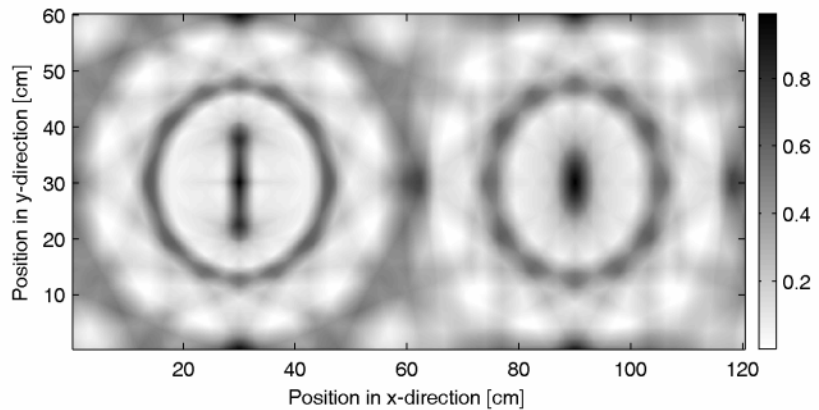
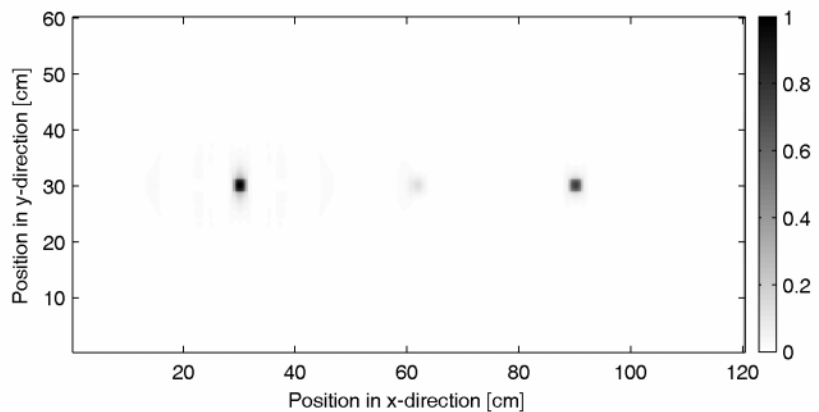


Fig. 4: Results of the new automated pin-pointing algorithm, equation (1), with  $n=20$  cm. Both objects are found. The pin-pointing is sharp and accurate.



### 2.3 Results for a real data set

The algorithm for automated pin-pointing is further evaluated for a 2d data set that was recorded on an outdoor test lane. These data sets put additional demands on the algorithm as they contain perturbations like sensor drift, sensor noise and soil fluctuations.

The measurements were carried out in Ispra [2] by the Fraunhofer Institute IZFP. A differential CW metal detector with an excitation frequency of 2.4 kHz was deployed. The data set was digitized nearby the receiving coil connector. The metal detector itself was mounted on an x-y-scanner that was moved on a zigzag pattern over the test field.

In Fig. 5, the data set for soil “4A” is shown. Again, signals with typical symmetry properties are perceptible (the buried metallic objects are near to the crosses of the additional grid). The positions that are the outcome of the pin-pointing algorithm are marked with numbered dots.

As expected, the algorithm detects weak signals that are difficult to detect otherwise (object 7; surrogate M1A at 5 cm depth). However, the limit is reached for surrogate M1A at greater depths that are neither accessible by symmetry or threshold algorithms. The object 4 is an unknown shrapnel piece that would not have been found by the classic threshold approach.

Complex extended objects are not accessible by the symmetry algorithm as the signals around these objects may lack the typical symmetry. An example in Fig. 5 is the object with markers 11 & 15, which in reality is one single object. However, with the strong signal in this example, the object is easily found by threshold methods. – The algorithm could generate false alarm, see e.g. object marker 5. Here, the detected symmetry lies exactly in the middle between two dominating objects. However, it could be eliminated by an extended version of the algorithm.

The result of this evaluation is that the algorithm works well with typical signal perturbations that occur in real data sets. The algorithm is a good supplement to threshold based methods.

### 3 Characteristic 2d phase values

When using a metal detector in a mine field, deminers use pin-pointing procedures to find the objects that probably could be a mine. The pin-pointing itself could be done manually or by an automatic algorithm as described in the previous chapter. The data sets in the proximity of a found object are now evaluated in more detail by calculating characteristic 2d phase values. In that way, additional information is provided to the deminer.

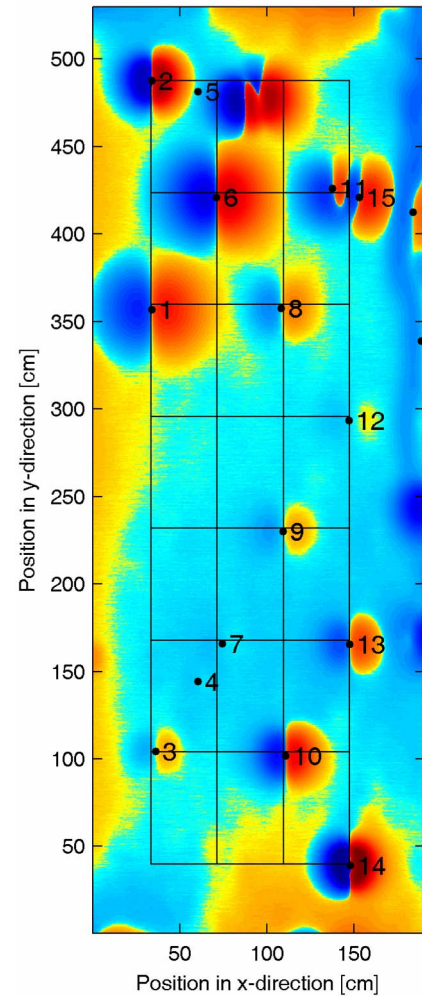


Fig. 5: The in-phase component for the soil “4A”, after conversion to a log-scale to enhance details. The grid serves as orientation help. The results of the automatic pin-pointing algorithm are marked with numbered dots.

### 3.1 Principle of the algorithm

In a first evaluation step, spatially resolved data sets around hidden objects are analyzed using concepts from the field of signal analysis. As in the previous chapter, the evaluation is based on simulated data sets that are calculated with a computer program from the University of Köln [8]. With that program, the detection process for different spheres is simulated by calculating the induction voltage of a receiving coil (real and imaginary parts), for different excitation frequencies in air. In the simulations, perturbations effects like soil variations are disregarded.

A major result of the evaluations is that the quotients of different combinations of measurement channels (real or imaginary parts for different frequencies) do not change when the metal detector is swept over a sphere. That means that the quotient is independent of the offset between detector and object (see Fig. 6) as well as of the depth of the object. The quotient however is dependent of the radius, the electrical conductivity and the magnetic permeability of the sphere. For that reason, signal quotients could be used to discriminate the simulated objects. The same holds for the phase of (complex) signal values as, by definition, the phase is an inverse trigonometric function of the quotients.

However, a simple constant phase assumption for data sets around objects is not admissible. In practice, complex and huge objects may have phase values that change notable when the detector is swept over the object [7]. And it is in the nature of things that it is usually unknown whether a buried object has a sphere like shape or not.

Based on these results, the new algorithm for discriminating different objects considers the following principle: If and only if the phase values (of different signal combinations) vary only slightly in the proximity of a hidden object, multidimensional average phase value are calculated as an additional feature for object discrimination.

### 3.2 Description of the algorithm

The algorithm for calculating characteristic 2d phase values processes data sets that are acquired with a differential two frequency CW metal detector. The detector is swept over a pin-pointed object. During that movement, data vectors  $d_i = (re1_i, re2_i, im1_i, im2_i)$  are steadily recorded, with consecutive label  $i$ . Each data vector contains the real “re” and imaginary “im” part of the responses, for each of the two frequencies  $f1$  and  $f2$  (labelled by “1” and “2”). The signals at the pin-pointed position are used as reference, i.e. they are subtracted from the measured signal values in order to obtain the signals in the vectors  $d_i$ .

In a first step, the influence of the soil is reduced. The soil influence is especially prevalent in the imaginary channels as it is shown in [11]. A simple method to reduce the soil influence is to transform the data  $\tilde{d}_i = (re1_i, re2_i, (f2/f1) \cdot im1_i - im2_i)$ . Also, more sophisticated methods for soil reduction could be applied. After this step, the data vectors are transformed to spherical coordinates, i.e.  $\hat{d}_i = (r_i, \theta_i, \vartheta_i)$ . To obtain proper phase values (in the context of complex signals) the values for  $\theta_i$  and  $\vartheta_i$  are constrained to a half space.

Subsequently, the variations of the phase values are evaluated. If they are below a threshold, characteristic 2d phase values  $\theta_{ch}$  and  $\vartheta_{ch}$  are calculated. To minimize noise effects, only the phase values of strong signal  $r_i$  are considered. When the data sets are spatially referenced, the allowed data vectors could be further confined to the positions where the signal extremes are expected.

$$\begin{pmatrix} \theta_{ch} \\ \vartheta_{ch} \end{pmatrix} = \begin{pmatrix} \text{mean}(\{\theta_i | r_i > r_{\min}\}) \\ \text{mean}(\{\vartheta_i | r_i > r_{\min}\}) \end{pmatrix} \quad (3)$$

The extension to data sets from multi-frequency CW metal detectors is straightforward.

### 3.3 Results for simulated 2d data sets

The new algorithm is evaluated using data sets from numerical simulations, similar to the procedure in the previous chapter. The simulation objects are different steel spheres, with diameters ranging from 4 mm to 36 mm. They are positioned in different depths from 20 mm up to 200 mm. The excitation frequencies are 2.4 kHz and 19.2 kHz. The induction values are computed for a straight line over the pin-pointed position, with a spacing of 1 mm. The results for simulated data sets are shown in Fig. 6.

The characteristic 2d phase values are an efficient feature to discriminate different spheres. The results for the same sphere at different depths lie on top of each other, i.e. the feature is indeed independent of the depth. Moreover, and especially important in the context of humanitarian demining, the object discrimination is well suited for small objects due to the enlarged spacing between the 2d phase values for small spheres.

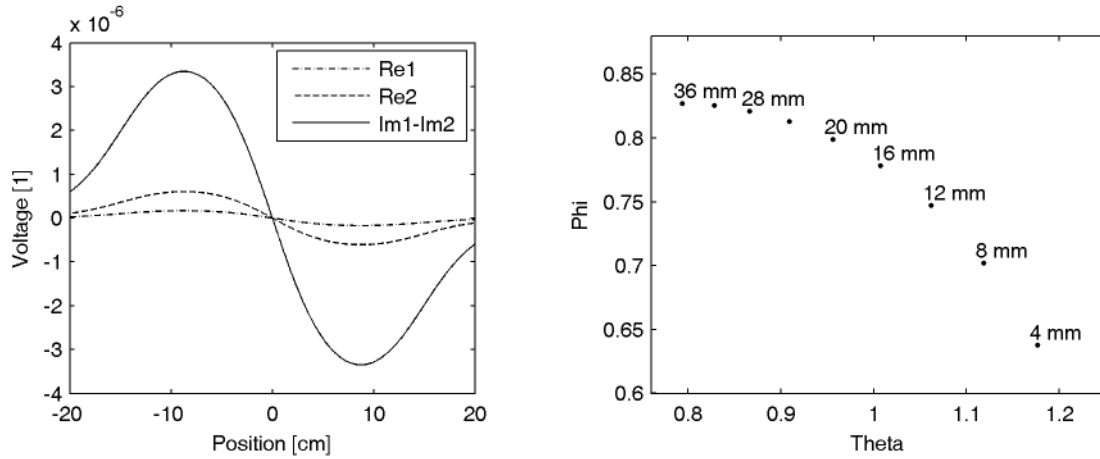


Fig. 6: Left: Simulated induction data for a sphere. The quotient of different responses (e.g. Re1/Re2) is independent of the position (x-axis) – Right: Characteristic 2d phase values for simulated steel spheres with different radii. The material parameters are  $\mu_r = 400$  and  $\sigma = 5.46$  MS/m.

### 3.4 Results for a real data set

The algorithm for automated pin-pointing is further evaluated for a real data set. The data set was recorded at the test site of the University of Rostock [5]. At this facility, steel spheres of different diameters as well as different mine surrogates (M1A and M2B) were buried in a loessic soil at depths ranging from 20 mm up to 200 mm. The measurements were carried out with a differential CW metal detector, with excitation frequencies of 2.4 kHz and 19.2 kHz. The data set was digitized nearby the receiving coil connector. The metal detector itself was mounted on an x-y-scanner that was moved on a zigzag pattern over the test field.

In a first step, the data sets are searched for metal objects using the pin-pointing algorithm from chapter 2. Objects with high metal content are found in all buried depths. Low metal objects, however, like the mine surrogate M1B, are only found up to a maximum detection depth, that is object depending and less than 200 mm.

All found objects are analyzed with the algorithm that provides characteristic 2d phase values. Although the signals measured on test lanes contain perturbations from

different sources like soil variations and sensor noise, the phase values are still almost independent of the offset between detector and buried object. In Fig. 7, the resulting characteristic 2d phase values of the algorithm are shown.

As a major result, the characteristic 2d phase values are a qualified means to exclude unknown objects from being a mine, at least for the evaluated objects. In Fig. 7, the values for one kind of object at different depths lie close together which is highlighted by grey boxes. As the boxes are non-overlapping, the characteristic phase values are features that allow for object discrimination. Subsequently, an assignment to the two categories “object is possibly a mine” and “object is definitely not a mine” could be done by a classifier. As the cluster for different objects are far apart, standard algorithms for classification could be used like e.g. a NN-classifier.

The characteristic 2d phase values of the spheres are in good agreement with the values that were predicted by the simulations. Also, the spacing between the two small spheres is notable bigger than the spacing between the two big spheres. The more extended and complex objects M1A and M2B lie aside off the line that is defined by the different spheres.

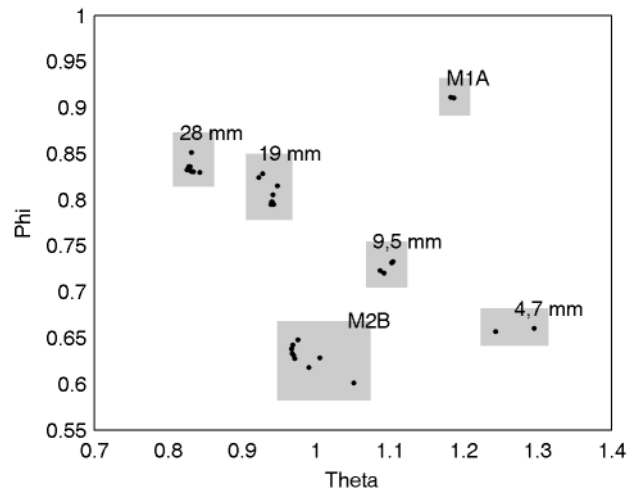


Fig. 7: Characteristic 2d phase values of different objects. All values for one single object are inside the labelled grey boxes. Each dot inside a box belongs to a different object depth (not inscribed).

## 4 Summary

In this article, new algorithms for the evaluation of CW metal detector data sets were presented. The algorithm for automatic pin-pointing provides reliable position estimations for metal objects in a test field. This is especially true in combination with classical threshold methods. At present, the algorithm requires data sets on a 2d grid as they are provided e.g. from an x-y-scanner. In order to integrate the symmetry concept to handheld metal detector, the amount of necessary input data still has to be reduced.

The algorithm for discriminating objects was tested for different objects that were successfully distinguished by the characteristic 2d phase values. At present, however, a generalisation of these results is difficult as the data basis so far is small. Additional measurements with more complex objects and different orientations will be necessary. The features are likely to vary more for complex and extended objects which is supported e.g. by the recorded data sets from Bruschini et al. [7]. The additional evaluations will also provide an indication whether this new method will be a candidate for a full integration with handheld metal detectors.



## 5 Acknowledgements

This work was supported by the Bundesministerium für Bildung und Forschung under Contract No. 01 RX 0308. I would like to thank Jörn Lange (University of Köln) and Tilman Hanstein (HarbourDom GmbH) for providing the simulation code.

## 6 References

- [1] D. Guelle, A. Smith, A. Lewis, T. Bloodworth, "Metal Detector Handbook for Humanitarian Demining", European Communities, Publication EUR 20837, 2003.
- [2] P. S. Verlinde, M. P. Acheroy, G. Nesti, A. J. Sieber, "First results of the joint multisensor mine-signatures measurement campaign", in Detection and Remediation Technologies for Mines and Minelike Targets VI, Proc. SPIE Vol. 4394, p. 1023-1034, 2001.
- [3] H.A. Lensen, "TNO test and evaluation facilities for landmine detection", Research on Demining Technologies Joint Workshop, Ispra, Italy, July 12–14, 2000.
- [4] C. Beumier, P. Druyts, Y. Yvinec, M. Acheroy, "Motion Estimation of a Hand-Held Mine Detector", Proc. 2nd IEEE Benelux Signal Processing Symposium (SPS-2000), Hilvarenbeek, March 23–24, 2000
- [5] H. Krueger, H. Ewald, Th. Fechner and S. Bergeler, "Advanced signal processing for reduction of false alarm rate of Metal detectors for humanitarian mine clearance", proceedings of IMTC 2006 -- Instrumentation and Measurement Technology Conference Sorrento, Italy 24-27 April 2006.
- [6] P. Szyngiera, "A Method of Metal Object Identification by Electromagnetic Means", in Proc. MINE'99, Mine Identification Novelties Euroconference, Florence, Italy, pp. 155-160, 1999.
- [7] C. Bruschini, L. van Kempen and J. Lochy, "Metal Target Discrimination with a Commercial Two Frequency Sensor - Part II: Quantitative Aspects," International Conference on Requirements and Technologies for the Detection, Removal and Neutralization of Landmines and UXO (EUDEM2-SCOT), vol. 1, pp. 304-311, Brussels, Belgium, 2003.
- [8] S. L. Helwig, T. Hanstein, A. Hördt, J. Lange, H. Ewald, H.-W. Glock, H. Krüger, Th. Krüger, S. Schulze, U. van Rienen, „Inversion von ortsaufgelösten Wirbelstrommessdaten zur Bestimmung der Lage und Geometrie von Landminen“, DGZfP Jahrestagung 2005, Rostock
- [9] D. Reisfeld, H. Wolfson, and Y. Yeshurum, "Detection of interest points using symmetry", Proc. Int. Conf. Computer Vision, Japan, Dec. 1990, pp. 62-65.
- [10] P. Kovese, "Symmetry and Asymmetry from Local Phase", AI'97, Tenth Australian Joint Conference on Artificial Intelligence, 2 - 4 December 1997, Proceedings, pp 185-190.
- [11] T. Hanstein, J. Lange, S. L. Helwig, „Der Einfluss (viskoser) magnetischer Böden auf Metalldetektoren“, 65. Jahrestagung der Deutschen Geophysikalischen Gesellschaft in Graz (2005), conference poster available at [http://www.geophysik.uni-koeln.de/forschung/humin/Hanstein\\_dgg05.pdf](http://www.geophysik.uni-koeln.de/forschung/humin/Hanstein_dgg05.pdf).